Peer-reviewed version available at Molecules 2018, 23, 23020273; doi:10.3390/molecules23020273

Article

Preparation, Characterization and Catalytic Activity of Nickel Molybdate $NiMoO_4$ Nanoparticles

Hicham Oudghiri-Hassani [1,2,*], and Fahd T. Al Wadaani[1]

[1]Taibah University, College of Science, Chemistry Department, Almadinah 30002 Saudia Arabia

[2]Cégep de Drummondville, Département Sciences de la nature, 960 rue Saint-Georges, Drummondville, Québec, Canada J2C 6A2

*Corresponding Author: Tel. +966543549454; *E-mail address*: oudghiri_hassani_hicham@yahoo.com

Abstract: Nickel molybdate, $NiMoO_4$, nanoparticles were synthesized via calcination of an oxalate complex in static air at 500 °C. The oxalate complex was analyzed by thermal gravimetric analysis (TGA) and Fourier transform infrared spectroscopy (FTIR). The as-synthesized nickel molybdate was characterized by Brunauer–Emmett–Teller technique (BET), X-ray diffraction (XRD), and transmission electron microscopy (TEM) and its catalytic efficiency was tested in the reduction reaction of the three-nitrophenol isomers. The nickel molybdate displays a very high activity in the catalytic reduction of the nitro functional group to an amino. The reduction progress was controlled using UV-Vis absorption.

Keywords: nickel molybdate; nanoparticles; catalysis; reduction of nitrophenol

1. Introduction

The increasing industrial activity produces effluents containing large amounts of organic pollutants such as paranitrophenol, which was classified as priority pollutant [1]. Its reduction will decrease its toxicity. Moreover, the reduction of the paranitrophenol to paraaminophenol is an important step in the industrial production of pharmaceutical analgesics such as paracetamol or acetaminophen (Figure 1) [2].

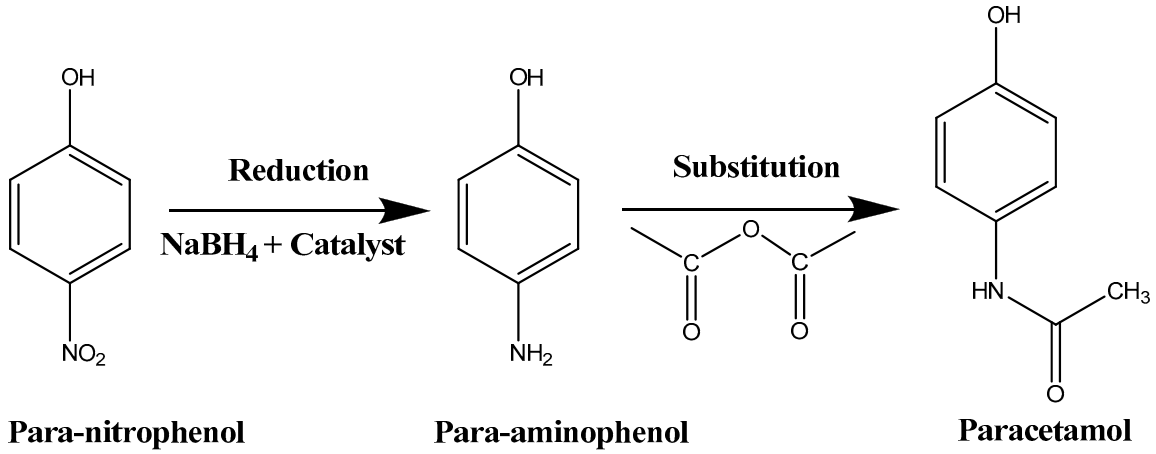

Figure 1. Schematic synthesis of the paracetamol from paranitrophenol.

The first step did not occur spontaneously, it requires the use of a catalyst. It becomes then useful and of interest to find a good and low cost catalyst that can be used in this reduction reaction.

Recently, Nickel molybdate ($NiMoO_4$) was intensively pursued because of its many applications. This promising compound was used as a catalyst for hydrodesulfurization and hydrodenitrogenation reactions [3, 4], oxidative dehydrogenation of light alkanes [5-9], partial oxidation of hydrocarbons [10], and microwave applications [11]. It was also used as a humidity

sensor [12], supercapacitor [13, 14], optical fibers, and military devices [15]. Nickel molybdate has attractive structures, electrochemical and magnetic properties [16, 17], and can be found in two crystalline forms, α-$NiMoO_4$ and β-$NiMoO_4$. Several methods were reported in literature to synthesize the nickel molybdate such as sonochemical [18, 19], hydrothermal [15, 20-21], precipitation [22, 23], sol–gel [22], mechanochemical synthesis [24], and solid state at high temperature [25, 26]. Different shapes were reported going from nanospherical, nanorodes to nanosheets [15, 21, 26, 27]. However, all of the previously reported methods required a strict reaction conditions, and high temperature or high pressure.

In this study, the nickel molybdate nanoparticles were synthesized using a new method and tested in the reduction of the three nitrophenol isomers (paranitrophenol 4-NP, metanitrophenol 3-NP and orthonitrophenol 2-NP). The results of the catalytic reaction tests are presented.

2. Experimental

2.1. Catalyst preparation

The nickel molybdate nanocatalyst was synthetized in two steps. First, a well-ground mixture of nickel nitrate $Ni(NO_3)_2{,}6H_2O$, ammonium molybdate $(NH_4)_6Mo_7O_{24}{,}4H_2O$, and oxalic acid $H_2C_2O_4{,}2H_2O$ in the molar ratio 1 /0.143 /10 [28] was used to obtain an oxalate precursor after heating at 160 °C. In fact, the oxalic acid was used in excess in order to reduce molybdenum and nitrate anions and to form a coordination complex of molybdenum and nickel. The appearance of light green color for the nickel molybdenum complex, and the production of the NO_2 gas (orange/brownish color) after heating at 160 C are results of the reduction reactions of molybdenum VI and the nitrate anion NO_3^- respectively. The last step was the thermal decomposition of the obtained nickel molybdenum complex for two hours under static air at 500 °C in a tubular furnace open both sides to obtain the nickel molybdate [29, 30].

2.2. Characterization

The precursor synthesized was analyzed by thermogravimetric analysis (TGA) and differential thermal analysis (DTA) using a SDT Q 600 instrument, and by FTIR using a Shimadzu 8400S apparatus at the frequency range of 400-4000 cm^{-1} using the sample that was prepared as KBr pellet. On other hand, X-ray diffractometer 6000, equipped with $\lambda_{Cu\text{-}K\alpha}$ =1.5406 Å with a Ni filter was used to identify the crystallized particles of the prepared nanocatalyst in the range of 10°–80° in 2θ. The Scherrer equation $D_{XRD} = 0.9\,\lambda/(B\cos\theta)$, was used to calculate the presumed spherical particle size, where θ is the Bragg angle, B is the full width at half maximum (FWHM) expressed in radians, and λ is the Cu-Kα wavelength. A Micromeritics ASAP 2020 surface area and porosity analyzer was used to measure the adsorption-desorption isotherms, and calculate the particle size with the following equation: $D_{BET} = 6000/d.S$ where S is the specific surface area, and d is the density.

A JEM – 1400 electron microscope was used to reach the shape and size of the particles, while the Varian Cary 100 spectrometer was used to measure the evolution of the solution concentration during the reduction reaction of the three-nitrophenol isomers.

2.3. Test of nitrophenol isomers reduction.

The reduction reaction of the three-nitrophenol isomers (4-NP, 3-NP, and 2-NP) was used to test the catalytic performance of nickel molybdate. In a typical test, 40 ml of the nitrophenol isomer aqueous solution 10^{-2} M was poured into, 40 ml of sodium tetrahydroborate $NaBH_4$ aqueous solution $2x10^{-2}$ M under continuous stirring at room temperature. A dark yellow color appears due to the formation of the nitrophenolate ion, and an absorption peak appears located at 401 nm, 393 nm, and 415 nm for 4-NP, 3-NP, and 2-NP respectively. The nickel molybdate nanocatalyst (0.1 g) was then added to the aqueous solution under stirring. The disappearance of the yellow color of the solution under the effect of the catalyst was followed by a UV-Vis spectrophotometer.

3. Results and discussion

3.1. Characterizations of the complex

The FTIR spectroscopy was used to identify the functional groups present in the complex synthesized by the solid-state reaction of the nickel nitrate, the ammonium molybdate and the oxalic acid, well ground mixture heated at 160 °C. In fact, the IR spectrum given in Figure 2 shows the presence of several wide bands. The deconvolution of these bands reveal, bands at 1738cm^{-1} and 1678 cm^{-1}, which can be assigned to the C=O vibration of the oxalate group [31]. This attribution is in accordance with the existence of the C-O stretch [31] located at 1400 cm^{-1}. While, both bands situated at 1361 and 1316 cm^{-1} can be assigned to υ(C-O) and δ(OCO) respectively [32]. At high frequencies the FTIR spectrum shows a band at 3398 cm^{-1} that corresponds to O-H bridging group between two metal ions [33], and two other bands at 3005 cm^{-1}, and 3195 cm^{-1}, which can be assigned to the stretching vibration of NH_4^+ ion [34]. However, the bands located at 1240 cm^{-1} and 1384 cm^{-1} can be assigned to δ(NH_4^+) [34], while that situated at 1638 cm^{-1} was attributed to δ(H_2O) [35]. In the other hand, the spectrum shows also, the Mo=O stretch [31] via the presence of the bands at 924 cm^{-1}, and 962 cm^{-1}. These results confirm the existence of the functional groups of oxalate, hydroxyl (-OH), water, oxo (Mo=O), and NH_4^+ ion in the synthesized complex.

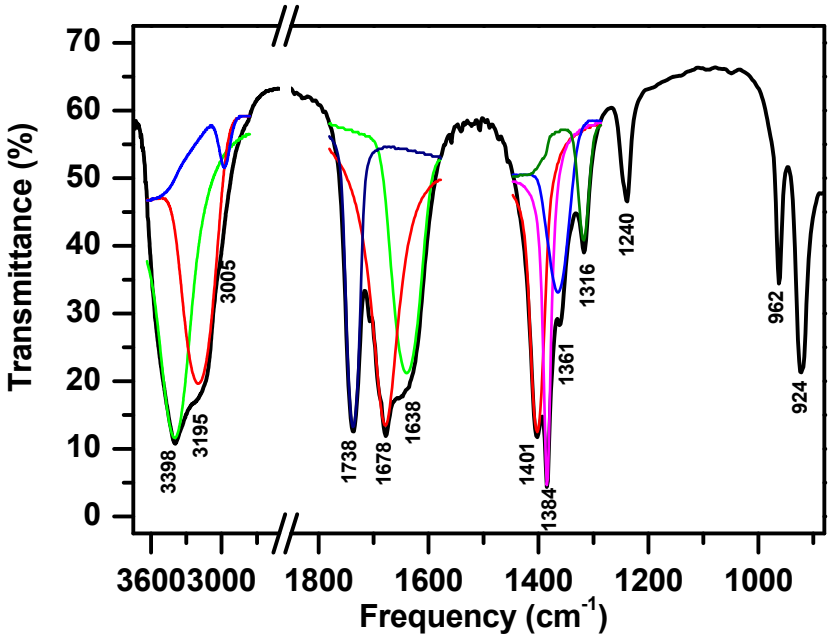

Fig. 2. Fourier transform infrared spectrum of the synthesized complex.

The thermogravimetric analysis was used in static air on the obtained complex, and recorded (Figure 3). The recorded curve can be divided in four parts. In the first part, a 4.5% weight loss was observed until 150 °C, which can be due to water molecules existing in the complex, confirmed by infrared spectroscopy studies reported above. In the second and third parts, a strongly and rapid exothermic loss occurs between 150 and 350 °C corresponding to the decomposition of the complex. In the fourth and last part, the curve shows a small and final loss between 350 and 450 °C. A similar loss in the same range that was also obtained in the previous study of bismuth oxalate complex can be attributed to OH group [33]. By compiling the results obtained by FTIR, TGA and the possible oxidation degree of nickel and molybdenum, we can suggest that the formula of the oxalate complex is $(NH_4)NiMoO(C_2O_4)_2(OH).H_2O$. The total weight loss observed is 47% in comparison with the

theoretical value of 45.3% for the suggested formula. The temperature of 500 °C was chosen to obtain the nickel molybdate by the calcination of the complex in static air.

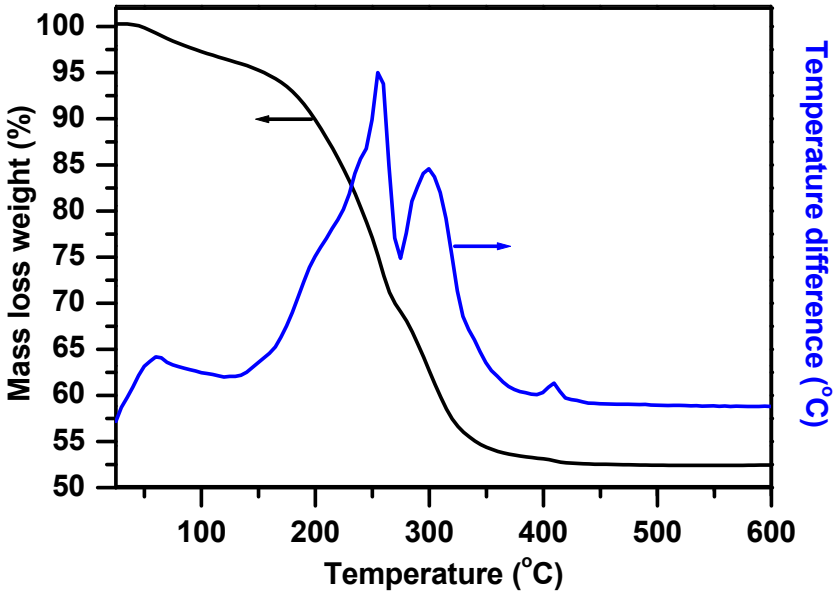

Fig. 3. Thermal gravimetric and thermal differential curves of the synthesized complex.

3.2. Nickel molybdate characterization

3.2.1 X- ray diffraction

The powder obtained after the calcination of the complex at 500 °C was analyzed by the XRD technique and the recorded pattern is presented in Figure 4. The XRD pattern is indexed in accordance with JCPDS file # 31-0902, which corresponds to the monoclinic phase α–$NiMoO_4$ that crystallizes in the space group C2/m (12) with the parameters a= 9.592 Å, b=8.755 Å, and c= 7.655 Å and β = 114.24°.

The two peaks located at 2θ =14.8° (110) and 2θ= 33.16° (310) were chosen to calculate the crystallites size D_{XRD}, which was found to be of 18 and 25 nm respectively.

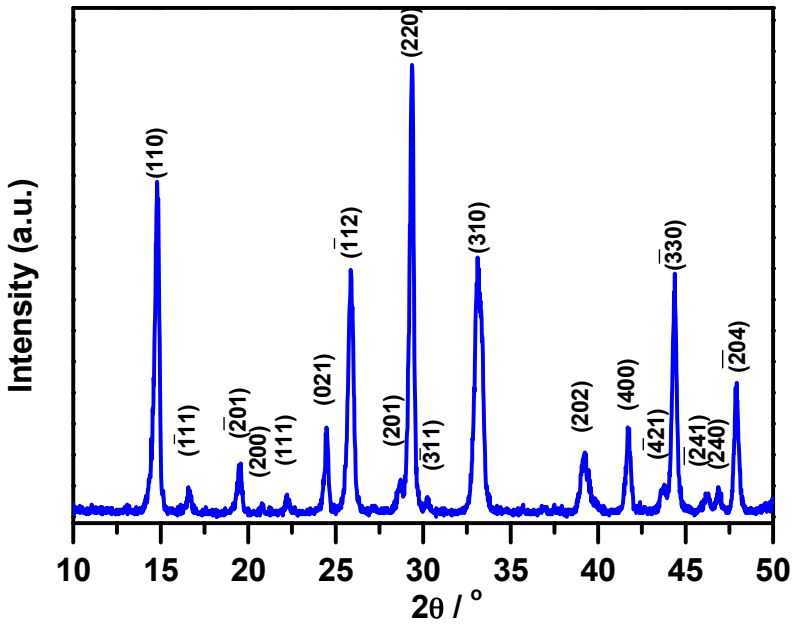

Fig. 4. X-ray diffraction pattern of the synthesized nickel molybdate.

3.2.2 Specific surface area determination

The specific surface area of the nickel molybdate $NiMoO_4$ synthetized by this simple method was estimated by the Brunauer–Emmett–Teller technique (BET). It was found to be of S_{BET} = 29.86 m^2/g. Knowing the value of the nickel molybdate density, d= 3.3723 g/cm^3, the particle size D_{BET} was calculated to be approximately 60 nm.

3.2.3 Transmission electron microscopy

The micrograph of the nickel molybdate prepared is shown in Figure 45. The particles are spherical and of 10 to 20 nm in size. However agglomerates of these nanoparticles of about 100 nm are formed.

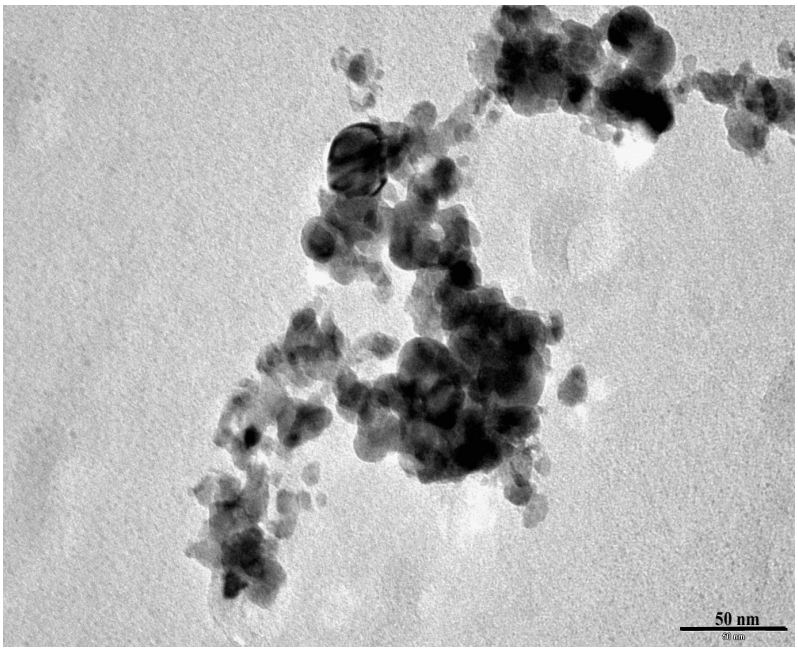

Fig. 5. Transmission electron microscopy micrograph of the synthesized nickel molybdate.

The calculations carried out with the XRD method on the first peak (110) show that the average size of the crystals is of 18, whereas the calculation carried out by the BET equation shows a size of approximately 60 nm. These results are consistent with the image recorded with the TEM despite the difference recorded. This can be explained by the fact that the BET technique has a lower nitrogen adsorption because of agglomeration, unlike the XRD technique where the calculations do not give the size of the particles but determine the size of the crystallites.

3.3. Reduction test of nitrophenol isomers

The reduction reaction of three nitrophenol isomers with $NaBH_4$ was investigated to test the catalytic efficiency of the successfully synthesized nickel molybdate (Figure 6 (a, b, and c)). Once the $NaBH_4$ was added, the nitrophenol isomers were converted to the NP ion nitrophenolate isomers (Figure 7). Before the addition of the as prepared catalyst, the dark yellow color of the solution stays unchanged during a period of 24 hours. However, after the addition of the nanocatalyst, the solution becomes uncolored in few minutes for all of the three-nitrophenol isomers. The higher peaks of absorption located at 401 nm, 393 nm, and 415 nm disappear in favor to new peaks situated at 317 nm, 328 nm, and 347 nm for the 4-NP, 3-NP and 2-NP, respectively. In fact, 8 min, 3 min, and 8 min were the necessary time to achieve the reaction with the appearance of the corresponding aminophenol isomers at room temperature. This result demonstrates the high catalytic efficiency of the synthesized nickel molybdate in the reduction of the nitrophenol isomers compared to previous research works found in the literature as presented in Table 1.

Table 1. A comparison of Reaction time for the reduction of 2-NP 3-NP and 4-Np by $NiMoO_4$ with other nanocatalysts reported in the literature.

Catalyst	Type	Concentration of NP (mol/L)	Reaction time (min)	References
$NiMoO_4$	Nanoparticles	5×10^{-3}	8 for 4NP 3 for 3NP 8 for 2NP	This work
$CuFe_2O_4$	Nanoparticles	3.6×10^{-2}	4 for 4NP 5 for 3NP 3 for 2NP	36
$NiFe_2O_4$	Nanoparticles	3.6×10^{-2}	38 for 4NP 36 for 3NP 28 for 2NP	36
CuO/ γAl_2O_3	Nanocomposites	2.9×10^{-5}	12 for 4NP 20 for 3NP 15 for 2NP	37
Ni/C black	Nanocomposites	5.0×10^{-4}	15 for 4NP 15 for 3NP 15 for 2NP	38

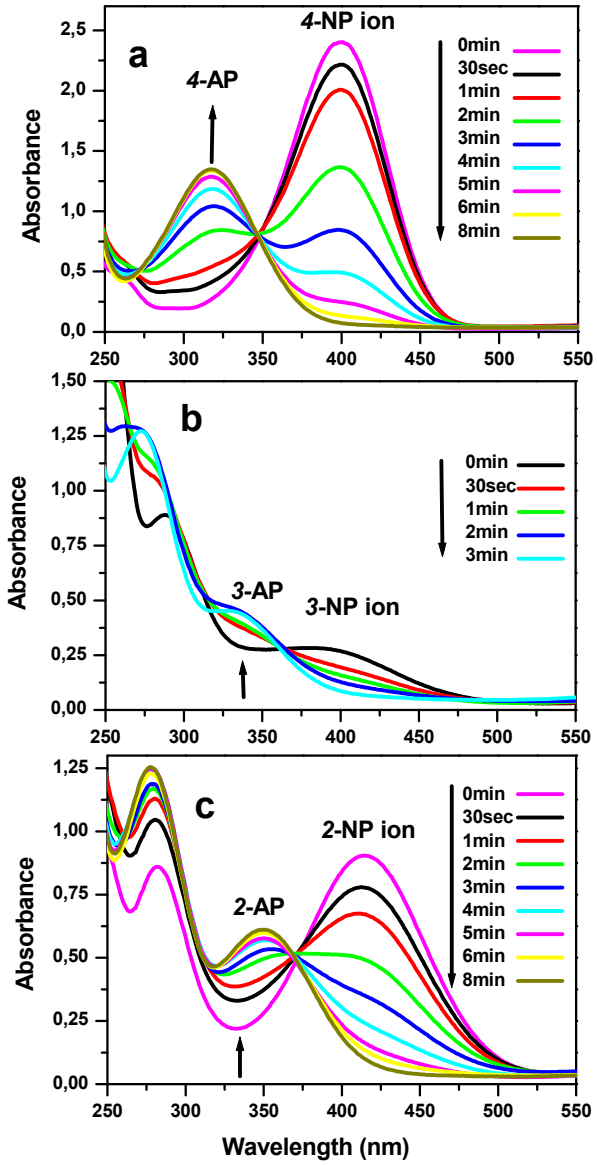

Fig. 6. UV-visible spectra of the reduction reaction solution of (a) 4-nitrophenol, (b) 3-nitrophenol, and (c) 2-nitrophenol in the presence of $NaBH_4$ using nickel molybdate.

Preprints (www.preprints.org) | NOT PEER-REVIEWED | Posted: 7 January 2018 doi:10.20944/preprints201801.0035.v1

Peer-reviewed version available at Molecules 2018, 23, 23020273; doi:10.3390/molecules23020273

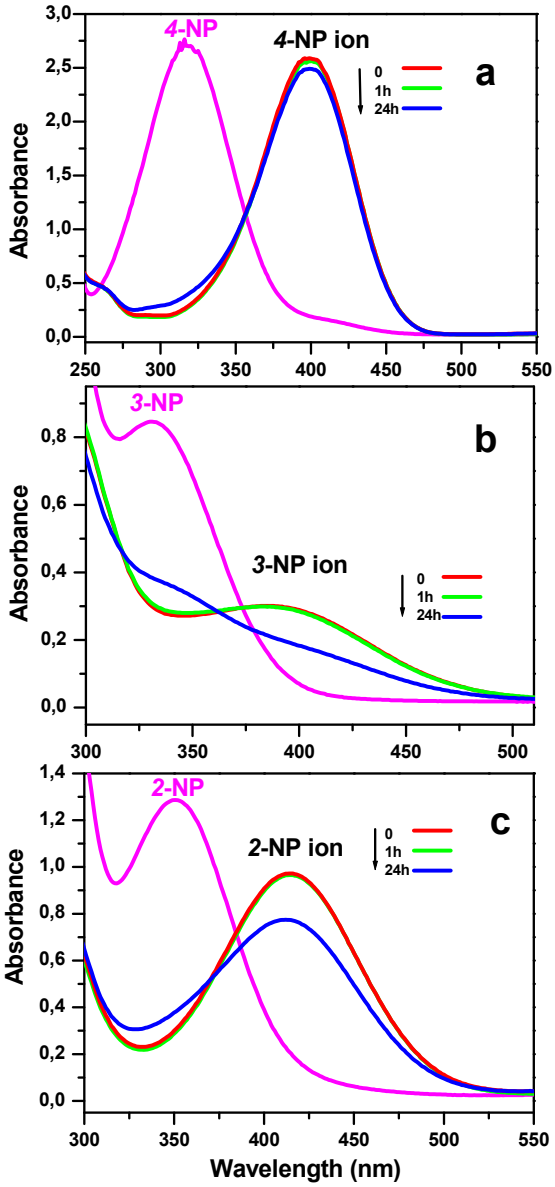

Fig. 7. UV–vis spectra of: (a) 4-nitrophenol, (b) 3-nitrophenol, and (c) 2-nitrophenol (NP) isomers before and after adding $NaBH_4$.

A mechanism for this reduction reaction can be supposed as follows. The nickel molybdate nanoparticles (NiMoNPs) dissociated the BH_4^- to form NiMoNPs-H and NiMoNPs-BH_3^- as reactive intermediates (Eq. (1)) [39]. Afterward, these intermediates reduce the nitrophenol isomers by (Eqs. (2) and (3)). Six electrons are involved in the formation of the aminophenol isomers (APi) from the corresponding nitrophenol (NPi).

$$2\ \text{NiMoNPs} + BH_4^- \longleftrightarrow \text{NiMoNPs-H} + \text{NiMoNPs-}BH_3^- \quad (1)$$

$$6\ \text{NiMoNPs-H} + \text{NPi} \longrightarrow \text{APi} + 6\ \text{NiMoNPs} + 6\ H^+ \quad (2)$$

$$6\ \text{NiMoNPs-}BH_3^- + \text{NPi} \longrightarrow \text{APi} + 6\ \text{NiMoNPs} + 6\ BH_3 \quad (3)$$

4. Conclusion

The nickel molybdate, α-$NiMoO_4$, was satisfyingly prepared as nanoparticles using a new and simple method. The high efficiency of the as-prepared nanocatalyst was confirmed in the reduction of the 4-NP, 3-NP, and 2-NP nitrophenol isomers. The studied nickel molybdate can be presented as a potential catalyst candidate for the reduction of the nitro functional group to an amino group.

References

1. Shimazu, M.; Mulchandani, A.; Che, W.; Simultaneous degradation of organophosphorus pesticides and p-nitrophenol by a genetically engineered Moraxella sp. With surface-expressed organophosphorus hydrolase. *Biotechnol. Bioeng.* **2001**, *76*, 318–324.
2. Espinosa Bosch, M.; Ruiz Sánchez, A.J.; Sánchez Rojas, F.; Bosch Ojeda, C.; Determination of paracetamol: Historical evolution. *J. Pharmaceut. Biomed.* **2006**, *42*, 291-321.
3. Madeley, R.A.; Wanke, S.; Variation of the dispersion of active phases in commercial nickel-molybdenum/ -alumina hydrotreating catalysts during oxidative regeneration. *Appl. Catal.* 1988, *39*, 295–314.
4. Gates, B.C.; Katzer, J.R.; Schuit, G.C.A.; Chemistry of Catalytic Processes, McGraw-Hill, New York, **1979**, p. 390.
5. Kaddouri, A.; Anouchinsky, R.; Mazzocchia, C.; Madeira, L.M.; Portela, M.F.; Oxidative dehydrogenation of ethane on the α and β phases of $NiMoO_4$. *Catal. Today* **1998**, *40*, 201–206.
6. Pillay, B.; Mathebula, M.R.; Friedrich, H.B.; The oxidative dehydrogenation of *n*-hexane over Ni–Mo–O catalysts. *Appl. Catal. A*. **2009**, *361*, 57–64.
7. Rodriguez, J.A.; Chaturvedi, S.; Hanson, J.C.; Brito, J.L.; Reaction of H_2 and H_2S with $CoMoO_4$ and $NiMoO_4$: TPR, XANES, Time-Resolved XRD, and Molecular-Orbital Studies. *J. Phys. Chem.* 1999, *103*, **770 –**
8. Sundaram, R.; Nagaraja, K.S.; Solid state electrical conductivity and humidity sensing studies on metal molybdate–molybdenum trioxide composites (M = Ni^{2+}, Cu^{2+} and Pb^{2+}). *Sens. Actuators B Chem*. 2004, *101*, 353-360.
9. Mi, Y.; Huang, Z.; Hu, F.; Jiang, J.; Li, Y.; Controlled synthesis and growth mechanism of alpha nickel molybate microhombohedron. *Mater. Lett.* 2010, *64*, 695-697.
10. Brito, J.L.; Barbosa, A.L.; Albornoz, A.; Severino, F.; Nickel molybdate as precursor of HDS catalysts: effect of phase composition. *Catal. Lett.* **1994**, *26*, 329-337.
11. Ryu, J.H.; Koo, S.M.; Yoon, J.W.; Lim, C.S.; Shim, K.B.; Synthesis of nanocrystalline $MMoO_4$ (M=Ni, Zn) phosphors via a citrate complex route assisted by microwave irradiation and their photoluminescence. *Mater. Lett.* **2006**, *60*, 1702-1705.
12. Chen, Y.; Meng, F.; Ma, C.; Yang, Z.; Zhu, C.; Ouyang, Q.; Gao, P.; Li, J.; Sun, C.; *In situ* diffusion growth of $Fe_2(MoO_4)_3$ nanocrystalson the surface of α-MoO_3 nanorods with significantly enhanced ethanol sensing properties. *J. Mater. Chem.* 2012, *22*, 12900-12906.
13. Senthilkumar, B.; Vijaya Sankar, K.; Selvan, R.K.; Danielle, M.; Manickam, M.; Nano α-$NiMoO_4$ as a new electrode for electrochemical supercapacitors. *RSC Adv.* 2013, *3*, 352-357.
14. Liu, M. Kong, L.; Lu, C.; Li, X.; Luo, Y.; Kang, L.; Waste paper based activated carbon monolith as electrode materials for high performance electric double-layer capacitors. *RSC Adv.* 2012, *2*, 1890-1896.
15. P. Liu, Y. Deng, Q. Zhang, Z. Hu, Z. Xu, Y. Liu, M. Yao, Z. Ai, Facile synthesis and characterization of high-performance $NiMoO_4{\cdot}xH_2O$ nanorods electrode material for supercapacitors. *Ionics.* 2015, *21*, 2797-2804.
16. Cherian, C.T.; Reddy, M.V.; Haur, S.C.; Chowdari, B.V.R.; Interconnected Network of $CoMoO_4$ Submicrometer Particles As High Capacity Anode Material for Lithium Ion Batteries. *ACS Appl Mater. Interfaces* 2013, *5*, 918-923.
17. Ding, Y.; Yu, S.H.; Liu, C.; Zang, Z.A.; 3D Architectures of Iron Molybdate: Phase Selective Synthesis, Growth Mechanism, and Magnetic Properties. *Chem. Eur. J.* 2007, *13*, 746-753.
18. Saberyan, K.; Soofivand, F.; Kianpour, G.; Salavati-Niasari, M.; Bagheri, S.; Synthesis and characterization of $NiMoO_4$ via ultrasonic route by a novel precursor. *J. Mater. Sci. Mater. Electron.* **2016,** *27*, 3765-3772.
19. Kianpour, G.; Salavati-Niasari, M.; Emadi, H.; Sonochemical synthesis and characterization of $NiMoO_4$ nanorods. *Ultrason. Sonochem.* 2013, *20*, 418-424.
20. Cai, D.; Wang, D.; Liu, B.; Wang, Y.; Liu, Y.; Wang, L.; Li, H.; Li, H.Q.; Wang, T.; Comparison of the Electrochemical Performance of $NiMoO_4$ Nanorods and Hierarchical Nanospheres for Supercapacitor Applications. *ACS Appl. Mater. Interfaces* **2013,** *5*, 12905-12910.

21. Ray, S.K.; Dipesh, D.; Yuwaraj, K. K.; Soo, W.L.; Cu- -$NiMoO_4$ photocatalyst for degradation of Methylene blue with pathways and antibacterial performance. *J. Photoch. Photobio. A.* **2017**, *348 (1)*, 18-32.
22. Kaddouri, A.; Tempesti, E.; Mazzocchia, C.; Comparative study of β-nickel molybdate phase obtained by conventional precipitation and the sol-gel method.*Mater. Res. Bull.* **2004,** *39(4–5),* 695-706.
23. Mosleh, M.; Facile approach to synthesize nanocristalline $NiMoO_4$ in the presence of amino acids as capping agent. *J Mater Sci: Mater Electron*. **2017**, *28*, 6788–6793.
24. Klissurski, D.; Mancheva, M.; Iordanova, R.; Kunev, B.; Mechanochemical Synthesis of Nanocrystalline Nickel Molybdates. *J. Alloy. Compd*. 2006, *422*, 53-57.
25. Maione, A.; Devilers M.; Solid Solutions of Ni and Co Molybdates in Silica-Dispersed and Bulk Catalysts Prepared by Sol-Gel and Citrate Methods. *J. Solid State Chem.* **2004,** *177*, 2339-2349.
26. Ramachandran, S.; P.; Ravi, G.; Ganesh, V.; Sakunthala, A.; Yuvakkumar, R.; Morphology dependent electrochemical capacitor performance of $NiMoO_4$ nanoparticles. *Mater. Lett. 209*, 2017, 1-4.
27. Cai, D. ; Liu, B. ; Wang, D. ; Liu, Y. ; Wang, L.; Li, H.; Wang, Y.; Wang, C.; Li, Q. ; Wang, T.; Enhanced performance of supercapacitors with ultrathin mesoporous $NiMoO_4$ nanosheets. *Electrochim. Acta*. 2014, 125, 294-301.
28. Oudghiri-Hassani, H.; Synthesis, characterization and catalytic performance of iron molybdate $Fe_2(MoO_4)_3$ nanoparticles. *Catal. Commun.* 2015, *60*, 19–22.
29. Abboudi, M.; Messali, M.; Kadiri, N.; Ben Ali, A.; Moran, E.; Synthesis of CuO, La_2O_3, and La_2CuO_4 by the Thermal-Decomposition of Oxalates Precursors Using a New Method. *Synth. React. Inorg. Met.-Org. Chem.* 2011, *41*, 683-688.
30. Messali, M.; Al Wadaani, F.; Oudghiri-Hassani, H.; Rakass, S.; Al Amri, S.; Benaissa, M.; Abboudi, M.; Preparation, characterization and photocatalytic activity of hexagonal ZnO nanoparticles. *Mater. Lett.* 2014, *128*, 187-190.
31. K. Nakamoto, Infrared and Raman Spectra of Inorganic and Coordination Compounds Part B: Applications in Coordination, Organometallic, and Bioinorganic Chemistry, 6th ed.; Wiley, New York, NY, USA, 2009, pp. 152-165, ISBN 978-0-471-74493-1.
32. Ng, K.; Y.; S.; Zhou, X.; Gulari, **E.;** Spectroscopic characterization of molybdenum oxalate in solution and on alumina. *J. Phys. Chem.* **1985,** *89*, 2477–2481
33. Rivenet, M.; Roussel, P.; Abraham, F.; One-dimensional inorganic arrangement in the bismuth oxalate hydroxide $Bi(C_2O_4)OH$, *J. Solid State Chem.* **2008,** *181*, 2586-2590.
34. Onodera, S.; Ikegami, Y.; Synthesis and properties of chlorine(I) and bromine(I) trifluoromethanesulfonates and Raman spectra of CF_3SO_2X (X=fluorine, hydroxyl, hypochlorite). *Inorg. Chem.* **1980,** *19*, 615-618.
35. Angermann, A.; Topfer, J.; Synthesis of nanocrystalline Mn–Zn ferrite powders through thermolysis of mixed oxalates. *Ceram. Int.* 2011, *37*, 995–1002.
36. Goyal, A.; Bansal, S.; Singhal, S.; Facile reduction of nitrophenols: Comparative catalytic efficiency of MFe_2O_4 (M = Ni, Cu, Zn) nano ferrites. *Int. J. Hydrogen Energ*. 2014, 39, 4895-4908.
37. Nandanwar, S.; U.; Chakraborty, M.; Synthesis of Colloidal CuO/γ-Al_2O_3 by Microemulsion and Its Catalytic Reduction of Aromatic Nitro Compounds. *Chinese J. Catal.* 2012, 33, 1532-1541.
38. Xia, J.; He, G.; Zhang, L.; Sun, X.; Wang, X.; Hydrogenation of nitrophenols catalyzed by carbon black-supported nickel nanoparticles under mild conditions. *Appl. Catal. B-Environ.* 2016, 180, 408-415.39. Holbrook, K.; A.; Twist, P.; J.; Hydrolysis of the Borohydride Ion catalysed by Metal-Boron Alloys. *J. Chem. Soc. A: Inorg. Phys. Theor.* **1971**, 890–894.